Short Article

Structure

Architecture of the Ubiquitylation Module of the Yeast Ccr4-Not Complex

Graphical Abstract

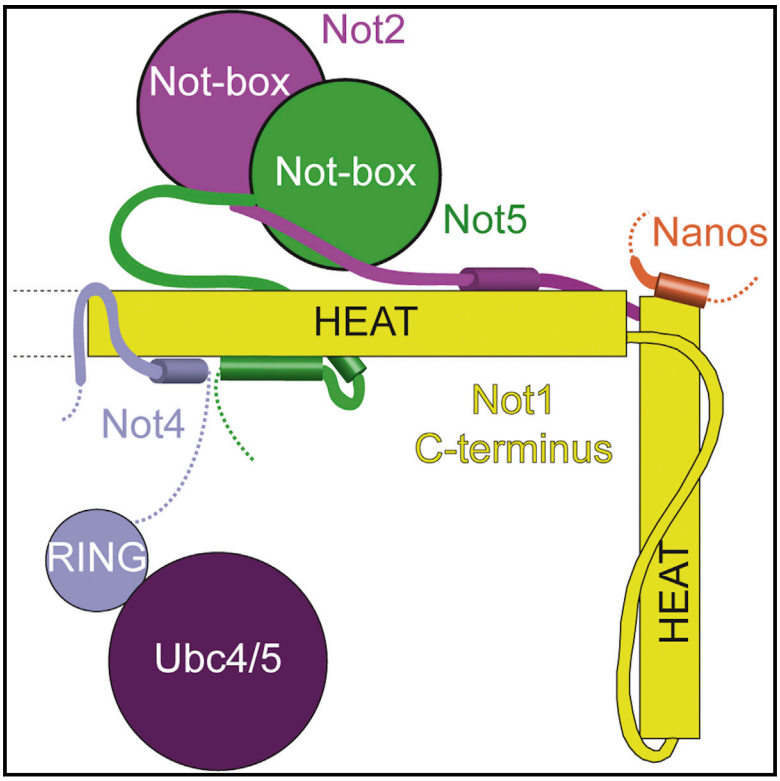

Authors

Varun Bhaskar, Jérôme Basquin, Elena Conti

Correspondence

conti@biochem.mpg.de

In Brief

Bhaskar et al. have determined the crystal structures of the complexes of the Not4 C-terminal domain with Not1 and the Not4 N-terminal RING domain with Ubc4. The structural and biochemical data highlight the underlying specificity of their interaction and rationalize the concomitant binding of Not4 and Not2-Not3/5 modules to Not1.

Highlights

- The Not1 C-terminal domain tethers the Not4 ubiquitylation module to yeast Ccr4-Not
- A low-complexity region of Not4 wraps around the C-terminal HEAT repeats of Not1
- In metazoans, Not4 lacks residues that confer high affinity binding to Not1 in yeast
- $Not1_C$ can recruit Not4 and Not2-Not5 concomitantly to the Ccr4-Not complex

Accession Numbers

5AIE
5AJD

Bhaskar et al., 2015, Structure *23*, 921–928
May 5, 2015
http://dx.doi.org/10.1016/j.str.2015.03.011

Structure
Short Article

Architecture of the Ubiquitylation Module of the Yeast Ccr4-Not Complex

Varun Bhaskar,[1] Jérôme Basquin,[1] and Elena Conti[1,*]
[1]Department of Structural Cell Biology, Max-Planck-Institute of Biochemistry, Am Klopferspitz 18, 82152 Munich, Germany
*Correspondence: conti@biochem.mpg.de
http://dx.doi.org/10.1016/j.str.2015.03.011

SUMMARY

The Ccr4-Not complex regulates eukaryotic gene expression at multiple levels, including mRNA turnover, translational repression, and transcription. We have studied the ubiquitylation module of the yeast Ccr4-Not complex and addressed how E3 ligase binds cognate E2 and how it is tethered to the complex. The 2.8-Å resolution crystal structure of the N-terminal RING domain of Not4 in complex with Ubc4 shows the detailed interactions of this E3-E2 complex. The 3.6-Å resolution crystal structure of the C-terminal domain of the yeast Not4 in complex with the C-terminal domain of Not1 reveals how a largely extended region at the C-terminus of Not4 wraps around a HEAT-repeat region of Not1. This C-terminal region of Not4 is only partly conserved in metazoans, rationalizing its weaker Not1-binding properties. The structural and biochemical data show how Not1 can incorporate both the ubiquitylation module and the Not2-Not3/5 module concomitantly in the Ccr4-Not complex.

INTRODUCTION

The Ccr4-Not complex is a crucial player in the regulation of eukaryotic gene expression (reviewed in Wahle and Winkler, 2013). Ccr4-Not was originally discovered as a transcriptional regulator in yeast (Collart and Struhl, 1994; Draper et al., 1994). Subsequent experiments revealed its fundamental function in cytoplasmic mRNA turnover, as a deadenylase that shortens the poly(A) tail at the 3′ end of mRNAs (Daugeron et al., 2001; Tucker et al., 2002). More recently, Ccr4-Not was also shown to act as a translational repressor (reviewed in Chapat and Corbo, 2014) and to be implicated in co-translational quality control (Panasenko, 2014; Matsuda et al., 2014).

Purification of the Ccr4-Not core complex from endogenous sources has revealed the presence of a large macromolecular assembly containing several evolutionary conserved proteins and a few proteins that are instead species specific (Chen et al., 2001; Lau et al., 2009; Temme et al., 2010; Erben et al., 2014). Ccr4-Not is assembled around Not1, a ~240 kDa protein that is built by consecutive helical domains. The individual domains of Not1 recruit the other core components of the complex forming structurally and functionally distinct modules. The Not1 N-terminal domain is an elongated HEAT-repeat fold (Basquin et al., 2012) and appears to bind species-specific subunits (CNOT10-CNOT11 in metazoans, Caf130 in yeast) (Chen et al., 2001; Mauxion et al., 2013; Bawankar et al., 2013). The Not1 central MIF4G domain is next and recruits Caf1 (also known as Pop2 in yeast) and Ccr4, forming the deadenylase module of the complex (Draper et al., 1994; Bai et al., 1999). This is followed by the Not1 helical bundle domain, which binds Caf40 (Bawankar et al., 2013). Last is the Not1 C-terminal domain, an elongated HEAT-repeat fold that binds Not2 and Not5 (and in yeast also the paralog Not3), forming the Not module of the complex (Bai et al., 1999). The C-terminal domain of Not1 also binds Not4, another core component of the yeast Ccr4-Not complex (Bai et al., 1999). Finally, several peripheral proteins are recruited to the core complex, such as DDX6, Nanos, tristetraprolin, and GW182 in metazoans (Maillet and Collart, 2002; Suzuki et al., 2010; Sandler et al., 2011; Braun et al., 2011; Chekulaeva et al., 2011; Fabian et al., 2011).

In the past few years, most of the conserved interactions of the core complex as well as the interactions with several peripheral factors have been elucidated at the structural level (Basquin et al., 2012; Petit et al., 2012; Fabian et al., 2013; Boland et al., 2013; Bhaskar et al., 2013; Bhandari et al., 2014; Chen et al., 2014; Mathys et al., 2014), with the exception of Not4. Not4 is an evolutionarily conserved protein that contains an N-terminal RING domain, a central RRM domain and a C-terminal domain predicted to be unstructured. As shown for both the yeast and human orthologs, the Not4 RING domain harbors an E3 ubiquitin ligase activity (Albert et al., 2002; Mulder et al., 2007a). Consistently, Not4 has been reported to ubiquitylate a wide range of substrates (Laribee et al., 2007; Mulder et al., 2007b; Mersman et al., 2009; Cooper et al., 2012; Gulshan et al., 2012), including ribosome-associated factors (Panasenko et al., 2006; Panasenko and Collart, 2012). Although the exact function is currently debated, the enzymatic activity of Not4 has been linked to proteasomal degradation in particular in the context of mRNA quality control pathways that respond to halted translation (Dimitrova et al., 2009; Matsuda et al., 2014). The activity of the Not4 E3 ligase depends on its interaction with a specific E2, which has been identified as Ubc4/5 in yeast and the ortholog UbcH5B in humans (Albert et al., 2002; Mulder et al., 2007a). Structural studies have shown how the RING domain of human CNOT4 folds via an unusual C4C4 motif whereby eight cysteine residues coordinate two zinc ions (Hanzawa et al., 2001). A model of the human CNOT4-UbcH5B complex has been proposed based on chemical shift nuclear magnetic resonance restraints,

computational docking approaches, and mutational analysis (Dominguez et al., 2004) but no crystal structure has been reported as yet.

Binding of yeast Not4 to the Ccr4-Not complex does not require the N-terminal RING domain but rather the C-terminal domain (Panasenko and Collart, 2011). The C-terminal domain of Not4, however, is the least conserved portion of the molecule. In addition, although Not4 is a bona fide Ccr4-Not subunit in yeast, it is not stably associated with the complex in human and *Drosophila* cells (Lau et al., 2009; Temme et al., 2010). The molecular basis for the Not1-Not4 interaction in yeast and the reason for the weaker association in higher eukaryotes are currently unknown. Also unknown is whether Not4 can bind Not1 in the context of the Not module, as Not2, Not3, and Not5 also dock to the same domain of Not1. Here, we report a structural and biochemical study that sheds light on how the E3 ligase of Not4 binds specifically its cognate E2 and how it is recruited to the Ccr4-Not complex.

RESULTS AND DISCUSSION

Overall Structure of *Saccharomyces cerevisiae* $Not4_N$ Bound to Ubc4

The N-terminal RING domain of Not4 ($Not4_N$, residues 30–83 in *S. cerevisiae*) has been shown to interact with Ubc4 (Figure 1A) (Albert et al., 2002; Mulder et al., 2007a). To obtain crystals of the complex, we used a strategy that had been reported for another E3-E2 complex (Hodson et al., 2014) and connected the two proteins covalently via a 10-residue linker. The structure of the $Not4_N$-Ubc4 fusion protein was determined by a combination of zinc-based single-wavelength anomalous dispersion (SAD) and molecular replacement, and was refined to 2.8-Å resolution with R_{free} of 27.1%, R_{factor} of 22.0%, and good stereochemistry (Table 1). The final model of $Not4_N$-Ubc4 has well-defined electron density for most of the polypeptide, except for the connecting linker (Figure 1B).

The structure of yeast $Not4_N$ bound to Ubc4 is very similar to that of the human CNOT4 ortholog in isolation (Hanzawa et al., 2001). The RING domain of Not4 contains two α-helices (the short α1 helix and the long α2 helix) and two zinc ions (Figure 1B). The zinc ions are coordinated in cross bracing fashion by cysteine residues that protrude from helix α2 and from the three loops regions L1, L2, and L3. The structure of yeast Ubc4 bound to $Not4_N$ is very similar to a previously determined structure of Ubc4 in isolation (Cook et al., 1993). Briefly, Ubc4 is centered at a four-stranded antiparallel β-sheet flanked by an N-terminal α-helix (α1) and by three C-terminal α-helices (α2, α3, α4) (Figure 1B). When compared with the previously proposed model of the human CNOT4-UbcH5B complex (Dominguez et al., 2004), the experimentally determined structure of yeast $Not4_N$-Ubc4 shows localized differences (Figure S1A).

Specific Interaction Network between the $Not4_N$ RING E3 and the Ubc4 E2

In the crystal structure, the Not4 helix α2 and the zinc-binding loops L1, L2, and L3 interact with two loops of Ubc4 that precede and follow the fourth strand of the β-sheet (L4 and L5) (Figure 1B). The central hotspot of the interaction is formed by Phe63 of Ubc4, which wedges into a hydrophobic pocket formed by Leu35, Ile56, Cys60, Asn63, Leu70, and Pro75 of Not4 and by Pro62 and Pro96 of Ubc4 (Figure 1C). In addition, Ile37 of Not4 is involved in hydrophobic interactions with the aliphatic portion of the side chain of Lys5 and Lys9 in the helix α1 of Ubc4. This hydrophobic hotspot is surrounded by polar and electrostatic contacts: a hydrogen-bond interaction involving Not4 Arg78 and Ubc4 Gln93 and two salt bridge interactions between Not4 Glu38 and Ubc4 Lys5 and between Not4 Glu69 and Ubc4 Lys64 (Figure 1C). In addition, Ubc4 Lys64 is engaged in an intra-molecular salt bridge with Ubc4 Asp60. The Glu69-Lys64-Asp60 network effectively pulls the L3 loop of Not4 toward Ubc4, closing the hydrophobic core. The interaction interface is formed by evolutionary conserved residues (Figures 1D and 1E) and is consistent with the effects of mutations previously reported (Mulder et al., 2007a).

To understand the specificity of yeast Not4 toward Ubc4/5 enzymes, we structurally aligned the known yeast E2 proteins on Ubc4 and analyzed if residues at the Not4-binding interface are conserved (Figure S1B). The Ubc2 and Ubc9 E2 proteins lack a hydrophobic residue at the corresponding position of Ubc4 Phe63. Ubc3, Ubc7, Ubc10, Ubc12, and Ubc13 lack a positively charged residue at the corresponding position of Ubc4 Lys64. Ubc1, Ubc6, Ubc8, and Ubc11 lack the equivalent of Ubc4 Gln93. These subtle differences appear to weaken the interaction network observed in the $Not4_N$-Ubc4 structure, driving the specificity of $Not4_N$ toward Ubc4/5 (Albert et al., 2002; Mulder et al., 2007a).

Overall Structure of $Not4_C$ Bound to $Not1_C$

The C-terminal domain of *S. cerevisiae* Not4 (specifically residues 430–480) has been shown to interact with the C-terminal domain of Not1 by yeast two-hybrid and co-immunoprecipitation (co-IP) studies (Albert et al., 2002; Panasenko and Collart, 2011). To ensure the identification of the correct domain boundaries that would include all the determinants of the interaction, we used secondary structure predictions to engineer larger regions of the interacting proteins than those mapped from the co-IP experiment. We purified a complex encompassing Not1 residues 1348–2093 and Not4 residues 418–587 (Not4 Δ417). Limited proteolysis of this complex and subsequent gel filtration resulted in stable fragments that were characterized by N-terminal sequencing and mass spectrometry analysis as encompassing residues 418–477 of Not4 ($Not4_C$) and residues 1541–2093 of Not1 (the C-terminal domain of Not1, or $Not1_C$) (Figures 2A and S2). Consistent with the proteolysis results, GST-tagged $Not4_C$ was able to precipitate $Not1_C$ in pull-down assays (Figure 2B, lane 3). We purified the $Not1_C$-$Not4_C$ minimal complex and obtained crystals diffracting to 3.6-Å resolution containing six copies of the complex in the asymmetric unit. We determined the structure by molecular replacement, using the previously determined structure of $Not1_C$ as the search model (Bhaskar et al., 2013). The model was built and refined to R_{free} of 31.9%, R_{factor} of 26.6%, and good stereochemistry (Table 1). The six independent copies of the complex in the crystals are essentially identical and include residues 1568–2078 of Not1 (with the major exception of two loops between 1791–1800 and 2065–2071) and residues 420–469 of Not4 (Figure 2C).

The HEAT-repeat structure of $Not1_C$ in the $Not4_C$-bound complex is similar to that in the Not2-$Not5_C$-bound complex (Bhaskar

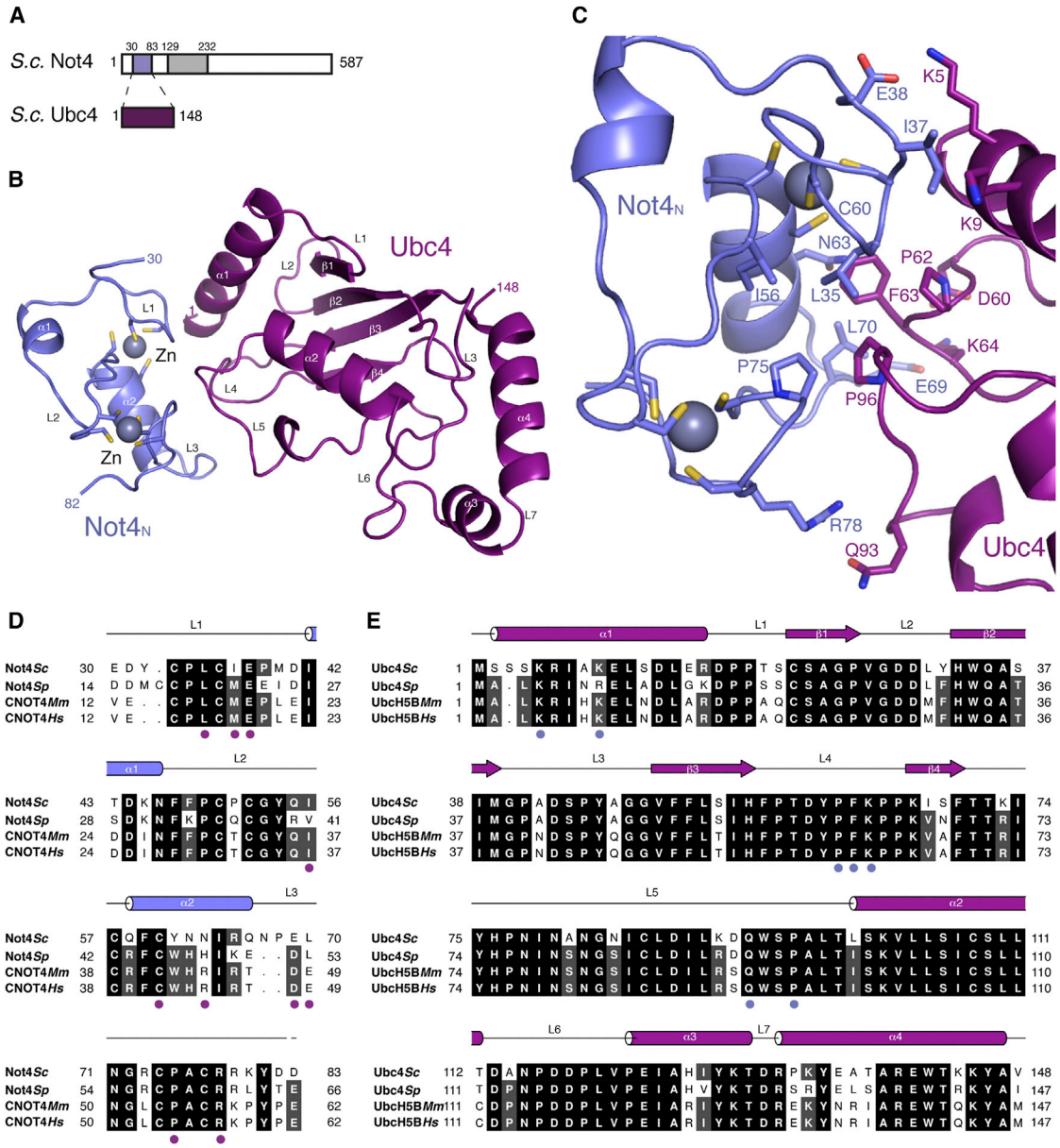

Figure 1. Structure of the Complex between the Not4 RING E3 and the Ubc4 E2

(A) A schematic diagram of the domain architecture of *S. cerevisiae* Not4 and Ubc4. The colored rectangles indicate the regions present in the crystal structure. The gray rectangle represents another folded domain, while the empty boxes represent low-complexity regions.

(B) Cartoon representation of the structure of yeast $Not4_N$ (in blue) bound to Ubc4 (in purple). The N- and C-terminal residues of the two proteins ordered in the electron density are indicated. The secondary structure elements are labeled. The two zinc ions are shown as spheres and the cysteine residues that coordinate them are shown in stick representation. This structure figure and all others in the article were generated using PyMOL (The PyMOL Molecular Graphics System, Version 1.2r3pre, Schrödinger, LLC).

(C) Close-up view of the interaction interface between $Not4_N$ and Ubc4. Interacting residues are shown and labeled.

(D and E) Structure-based sequence alignment of $Not4_N$ and Ubc4 from different species, including *S. cerevisiae* (*Sc*), *Mus musculus* (*Mm*) and *Homo sapiens* (*Hs*), highlighting the interacting residues. The secondary structure elements are shown above the sequence.

See also Figure S1.

et al., 2013). HEAT repeats consist of two antiparallel α-helices (termed A and B) and pack side by side in a regular fashion. The ten HEAT repeats of $Not1_C$ are organized in two units. The first unit is made of six HEAT repeats and is arranged in a perpendicular fashion with respect to the second unit, which is composed of the four C-terminal repeats (Figure 2C). The loop connecting HEATs 7 and 8 is in an extended conformation, likely due to crystal contacts. $Not4_C$ folds into an α-helix (residues 426–439) that is flanked by extended regions lacking defined secondary structure elements (residues 420–425 and 440–469) (Figure 2C).

Table 1. Data Collection and Refinement Statistics

	$Not4_N$-Ubc4		
	Zinc SAD	Native	$Not1_C$-$Not4_C$
Wavelength (Å)	1.2819	1	1
Resolution range (Å)[a]	37.33–2.48	53.56–2.80 (2.90–2.80)	75.66–3.62 (3.75–3.62)
Space group	*P1*	*R3H*	$P3_221$
Unit cell	62.45, 62.96, 65.43	107.11, 107.11, 62.20	173.66, 173.66, 262.61
α, β, γ (°)	108.50, 107.40, 108.09	90, 90, 120	90, 90, 120
Total reflections[a]	95,124 (13,582)	67,241 (6,289)	352,483 (34,067)
Unique reflections[a]	52,704 (7,634)	6,541 (628)	52,676 (5,095)
Multiplicity[a]	1.84 (1.77)	10.30 (10.00)	6.70 (6.70)
Completeness (%)[a]	92.5 (83.2)	99.4 (95.2)	99.7 (98.6)
Mean I/σ(I)[a]	14.66 (4.78)	29.35 (2.10)	11.26 (1.37)
SigAno[a]	1.31 (0.95)		
$CC_{1/2}$[a]	0.997 (0.949)	1 (0.911)	1 (0.733)
R_{merge} (%)[a]		5.6 (97.1)	11.2 (149.8)
R_{work} (%)[a]		22.0 (45.1)	26.6 (38.7)
R_{free} (%)[a]		27.1 (50.8)	31.9 (42.7)
Number of non-hydrogen atoms		1,575	24,555
Macromolecules		1,573	24,555
Ligands		2	0
Protein residues		204	3,223
RMS (bonds)		0.002	0.010
RMS (angles)		0.52	0.64
Ramachandran favored (%)		97	94
Ramachandran outliers (%)		0	0.064
Average B-factor		103.00	124.80
Macromolecules		103.10	124.80
Ligands		94.60	

SigAno = mean anomalous difference in units of its estimated standard deviation. (|F(+) − F(−)|/σ). F(+), F(−) are structure factor estimates obtained from the merged intensity observations in each parity class.
[a]Statistics for the highest-resolution shell are shown in parentheses.

Extensive Interaction Network between Yeast $Not1_C$ and $Not4_C$

$Not4_C$ binds on the surface of the first three HEAT repeats of $Not1_C$, extending about 100 Å in length and burying a surface area of approximately 1500 $Å^2$ (Figure 2C). The contacts between $Not4_C$ and $Not1_C$ can be described as divided into three segments. In the first segment, the α-helix of $Not4_C$ packs against the A helices of HEAT 2 and 3 of $Not1_C$. This interface is mainly dominated by hydrophobic interactions between Leu430, Leu434, and Leu437 of $Not4_C$ and Leu1613, Val1671, and Val1675 of $Not1_C$ (Figures 3A and S3A). In the second segment, residues 442–452 of Not4 interact extensively with two loops of $Not1_C$ connecting HEAT 1 to 2 and HEAT 2 to 3. The interactions are mediated by a salt bridge and few hydrophobic contacts (Figure 3B). In the third segment, residues 462–469 of Not4 are in extended conformation and pack between the A and B helices of the first HEAT repeat of $Not1_C$. This interface involves hydrophobic contacts between Leu463, Phe464, and Trp466 of Not4 and Val1575, Leu1582, Ile1592, Phe1596, Leu1600, and Val1605 of Not1 (Figures 3C and S3B).

To test the relevance of the interacting regions, we engineered deletion mutants of $Not4_C$ and carried out pull-down assays. As the second segment of the $Not1_C$-$Not4_C$ interface appeared the weakest from an analysis using the PISA server (Krissinel and Henrick, 2007), we constructed versions of $Not4_C$ lacking either the first hydrophobic segment ($Not4_C$-ΔN) or the C-terminal hydrophobic segment ($Not4_C$-ΔC). GST-tagged $Not4_C$-ΔN precipitated $Not1_C$ to a similar extent as GST-$Not4_C$ (Figure 3D, lanes 2 and 3). In contrast, GST-tagged $Not4_C$-ΔC failed to interact with $Not1_C$ in the pull-down assay (Figure 3D, lane 4). Next, we introduced specific mutations in the C-terminal segment of $Not4_C$ and tested them for their ability to interact with $Not1_C$ in GST pull-down assays. Mutations of $Not4_C$ either at Leu463 and Phe464 (L463E F464E) or at Phe464 and Trp466 (F464E W466E) failed to precipitate $Not1_C$ (Figure 3E, lanes 3 and 4). Altogether, these results suggest that the C-terminal segment of $Not4_C$ makes the most significant contribution to the Not1-Not4 interaction while the first and second segments of $Not4_C$ have a minor role.

Not4 Binding to Not1 Is Partially Conserved in Metazoa

To date, *S. cerevisiae* is the only species in which a stable association of Not4 within the Ccr4-Not core complex has been detected. This raises the question as to whether the interactions observed in the $Not1_C$-$Not4_C$ crystal structure are likely to occur in other species, particularly as in metazoa the incorporation of Not4 in the endogenous Ccr4-Not core complex has been barely detectable (Lau et al., 2009; Temme et al., 2010). In the case of Not1, many Not4-binding residues are evolutionarily conserved in higher eukaryotes (Figure S3C). In Not4, the first hydrophobic segment of the Not1-binding region is conserved. Human CNOT4, for example, features Ile419, Leu423, and Gln426 at the equivalent positions of *S. cerevisiae* Leu430, Leu434, and Leu437, respectively (Figure 3F). However, the third Not1-binding segment of Not4 is not present in human CNOT4. Since the third segment is essential for stable binding of Not4 to Not1 in yeast (Figures 3D and 3E), such differences rationalize the weaker in vivo association in higher eukaryotes (Lau et al., 2009; Temme et al., 2010).

Not4 Binding to Not1 Is Independent of the Not Module

Next, we compared the structure of the ubiquitylation module with that of the Not module. We superposed the structure of yeast $Not1_C$-$Not4_C$ with those of yeast $Not1_C$-Not2-$Not5_C$ (Bhaskar et al., 2013) and human $CNOT1_C$-$CNOT2_C$-$CNOT3_C$ (Boland et al., 2013). While $Not4_C$ binds the side surface of the first HEAT-repeat unit of $Not1_C$, yeast Not2-$Not5_C$ and human $CNOT2_C$-$CNOT3_C$ bind the top and the bottom surfaces (Figure 4A). Although there is a small overlap between the

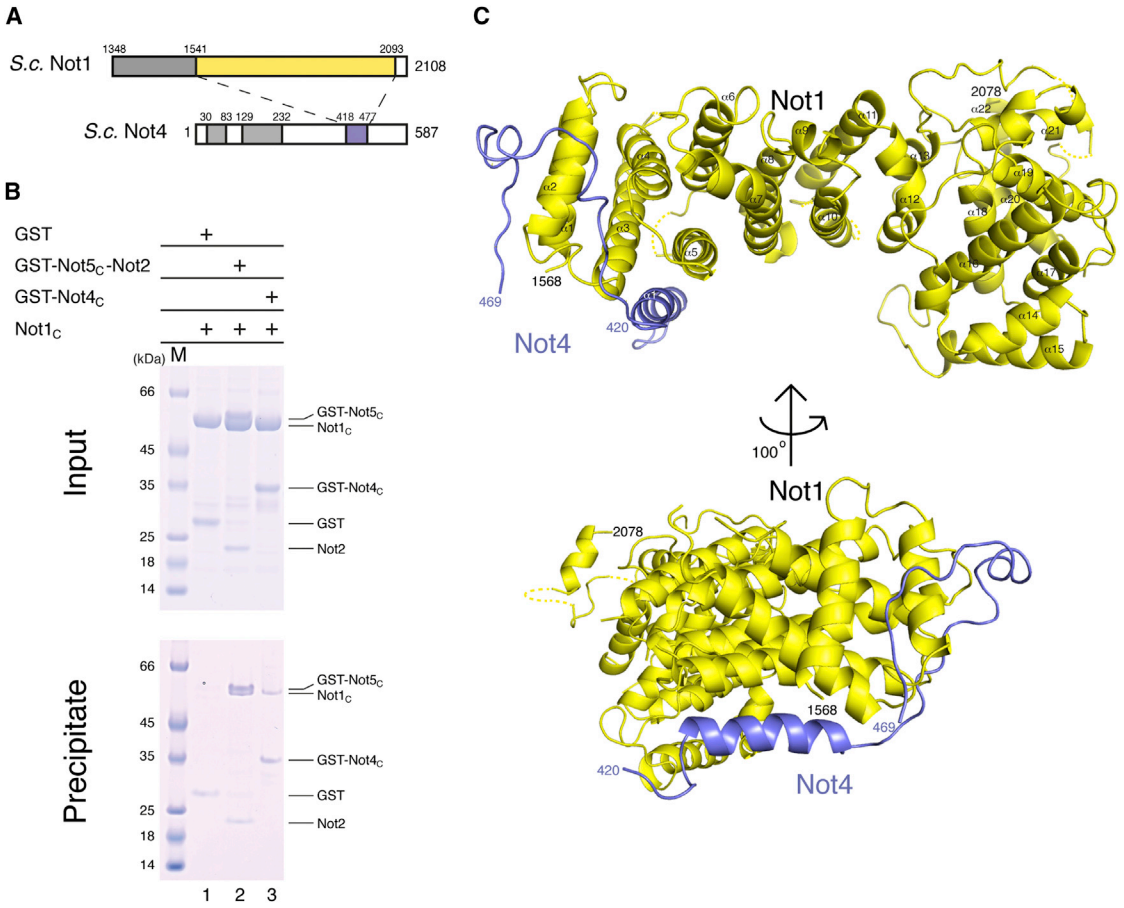

Figure 2. Structure of the Complex between Not4$_C$ and Not1$_C$

(A) A schematic diagram of the domain architecture of *S. cerevisiae* Not1 C-terminal region and Not4. The colored rectangles indicate the regions present in the structure. The gray rectangles represent other folded domains, while the empty boxes represent low-complexity regions.

(B) Protein co-precipitation by GST pull-down experiments. GST-Not4$_C$, GST-Not5$_C$-Not2 (positive control), or GST alone (negative control) were incubated with untagged Not1$_C$ in a buffer containing 150 mM NaCl before co-precipitation with GSH-Sepharose beads, as indicated. Input (upper panel) and precipitates (lower panel) were analyzed on Coomassie stained 4%–12% Bis-Tris gradient gel (NuPage, Invitrogen). The proteins are labeled on the right.

(C) Structure of the Not1$_C$-Not4$_C$ complex shown in cartoon representation in two orientations. Not1$_C$ is colored in yellow and Not4$_C$ in blue. The N- and C-terminal residues of both proteins are marked. Disordered loops are indicated as dotted lines.

See also Figure S2.

N-terminal helix of Not4$_C$ and the N-terminal region of Not5$_C$ as observed in the yeast Not1$_C$-Not2-Not5$_C$ complex, the structural analysis indicates that the interactions of Not4$_C$ and Not2-Not5$_C$ occur at largely separate surfaces of Not1$_C$. Indeed, pull-down assays showed that GST-tagged Not4$_C$ could precipitate Not2-Not5$_C$ in the presence of Not1$_C$ (Figure 4B). Thus, the ubiquitylation module and the Not module can form simultaneously on the C-terminal domain of Not1. Finally, Not4$_C$ binds at a completely different surface compared with the protein Nanos, which in metazoa is recognized by the C-terminal HEAT-repeat unit of CNOT1$_C$. Thus, the interactions of metazoan CNOT1 with CNOT2-CNOT3, CNOT4, and Nanos can in principle also occur simultaneously (Figure 4C). Whether and how bringing these proteins into close proximity by their concomitant interaction on the Not1$_C$ platform affects the regulation or coordination of their functions are open questions for future studies.

EXPERIMENTAL PROCEDURES

Protein Purification

All proteins were cloned, expressed, and purified as previously described (Bhaskar et al., 2013) (see Supplemental Experimental Procedures).

Crystallization and Structure Determination

All crystals were obtained by vapor diffusion at room temperature. All data were collected at the PXII and PXIII beamlines of the Swiss Light Source, processed using XDS (Kabsch, 2010), and scaled and merged using Aimless (Evans and Murshudov, 2013). The structures were obtained after iterative rounds of model building using the program Coot (Emsley et al., 2010) and/or BUCCANEER (Cowtan, 2006) and refined using PHENIX.REFINE (Adams et al., 2010). The Not4$_N$-Ubc4 complex was crystallized at 48 mg ml^{-1} (see Supplemental Experimental Procedures). Synchrotron data collected at the zinc edge (wavelength 1.28 Å) were used to solve the structure by molecular replacement-SAD in Phaser using the Ubc4 structure as a search model for molecular replacement and anomalous signal from the zinc atom (Cook et al., 1993; McCoy et al., 2007). The final

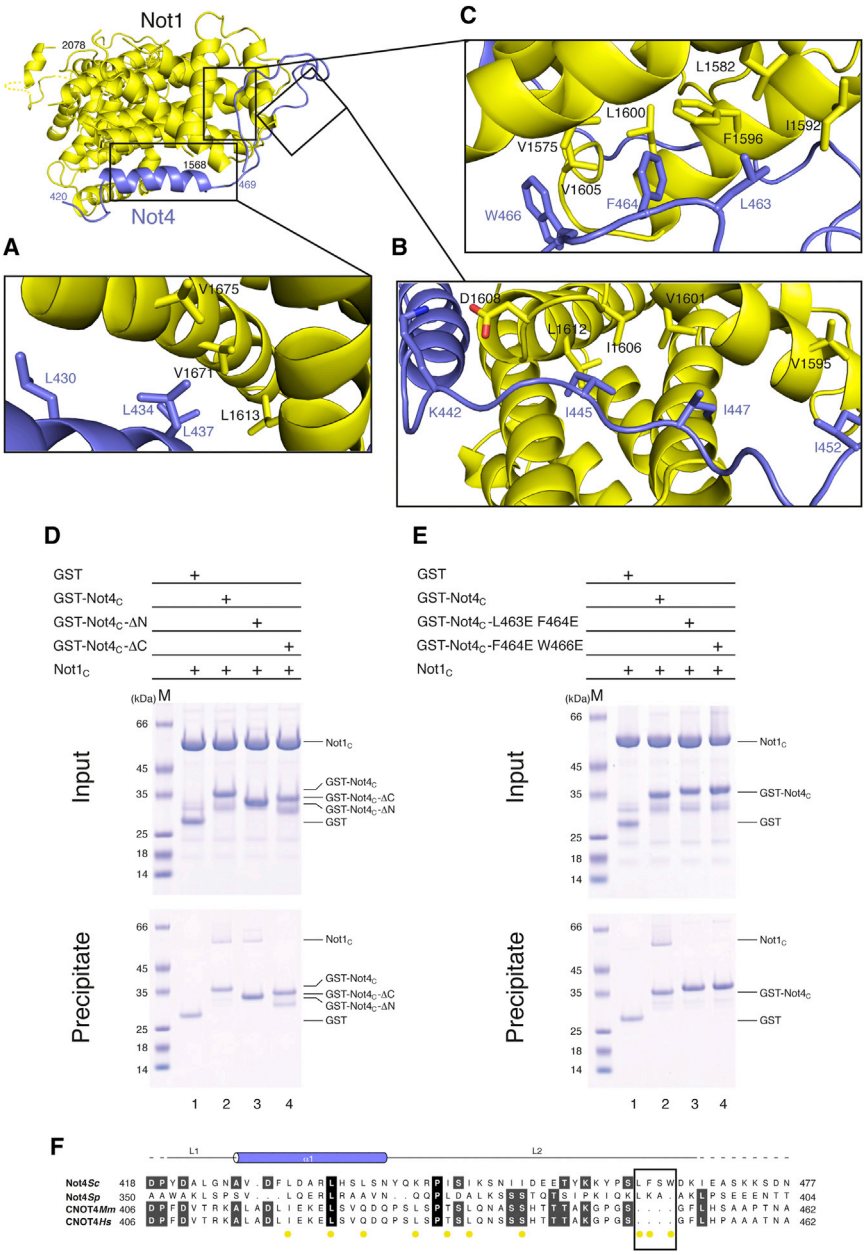

Figure 3. Not4$_C$ Wraps around the N-terminal HEAT Repeats of Not1$_C$

(A–C) Close-up view of different segments of Not4$_C$ that form the Not1$_C$ interacting region. The position of each individual segment in the context of the complex is shown on the top left. The residues involved in interactions are shown as sticks and labeled.

(D and E) Pull-down experiments with GST-tagged versions of Not4 and untagged Not1$_C$, carried out as described in Figure 2B.

(F) Structure-based sequence alignment of Not4$_C$ from different species, as mentioned in Figure 1D. The secondary structure elements are shown above the sequence.

See also Figure S3.

model was refined against a 2.8-Å resolution native dataset (collected at 1 Å wavelength).

Not1$_C$-Not4$_C$ was crystallized at 12 mg ml^{-1} (see Supplemental Experimental Procedures). The crystals belong to space group *P3$_2$21* with six copies in an asymmetric unit related by translational noncrystallographic symmetry (NCS). The structure was determined by molecular replacement using Not1$_C$ from the Not1$_C$-Not2-Not5$_C$ structure as the search model (Bhaskar et al., 2013). The model was refined for individual sites and individual B-factors along with torsion angle NCS restraints (in the initial rounds of refinement) that allow local conformational changes between the NCS-related copies.

Pull-down Assays

Pull-down assays of GST-tagged Not4 constructs with untagged Not1$_C$ and/or Not2-Not5$_C$ complex were performed as described in Bhaskar et al. (2013) (see Supplemental Experimental Procedures).

ACCESSION NUMBERS

The PDB accession numbers for the structure of Not4$_N$-Ubc4 and Not1$_C$-Not4$_C$ reported in this paper are 5AIE and 5AJD, respectively.

SUPPLEMENTAL INFORMATION

Supplemental Information includes Supplemental Experimental Procedure and three figures and can be found with this article online at http://dx.doi.org/10.1016/j.str.2015.03.011.

AUTHOR CONTRIBUTIONS

V.B. and J.B. performed the experiments; E.C. supervised the project; E.C. and V.B. wrote the manuscript.

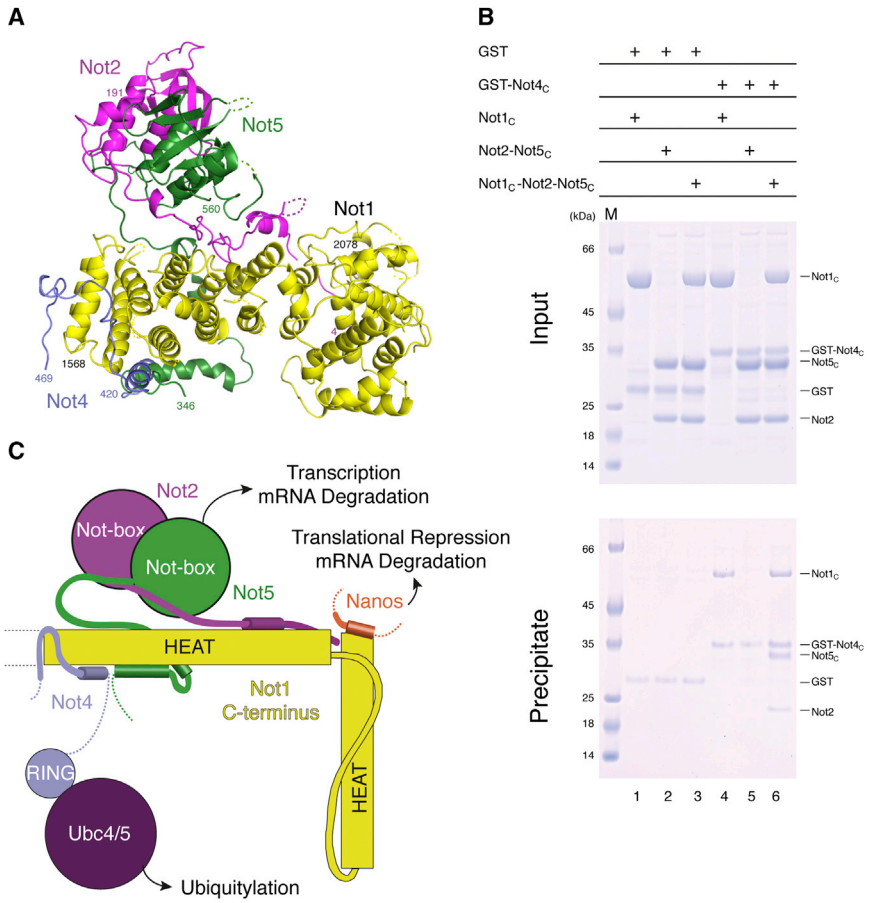

Figure 4. Not4$_C$ Binds Not1$_C$ Independently of Not2 and Not5

(A) Superposition of the yeast Not1$_C$-Not4$_C$ and Not1$_C$-Not2-Not5$_C$ structures. Not1$_C$ is in yellow, Not2 in magenta, Not5$_C$ in green, and Not4$_C$ in blue.

(B) Pull-down experiments with GST-tagged Not4$_C$ with untagged Not1$_C$ and/or Not2-Not5$_C$, carried out as described in Figure 2B.

(C) Schematic diagram of the C-terminal domain of Not1 with the positions of the interacting proteins Not4, Not2-Not5 (or CNOT2-CNOT3 in humans), and Nanos.

ACKNOWLEDGMENTS

We would like to thank the Max-Planck-Institute of Biochemistry Core Facility and Crystallization Facility; the staff members at the beamlines PXII and PXIII of the Swiss Light Source, Airlie McCoy and Pavel Afonine for suggestions on NCS treatment; members of our lab for useful discussions and critical reading of the manuscript. This study was supported by the Max-Planck Gesellschaft, the European Commission (ERC Advanced Investigator Grant 294371, Marie Curie ITN RNPnet), and the Deutsche Forschungsgemeinschaft (DFG SFB646, SFB1035, GRK1721, FOR1680, CIPSM) to E.C.

Received: January 9, 2015
Revised: March 12, 2015
Accepted: March 13, 2015
Published: April 23, 2015

REFERENCES

Adams, P.D., Afonine, P.V., Bunkóczi, G., Chen, V.B., Davis, I.W., Echols, N., Headd, J.J., Hung, L.-W., Kapral, G.J., Grosse-Kunstleve, R.W., et al. (2010). PHENIX: a comprehensive Python-based system for macromolecular structure solution. Acta Crystallogr. D Biol. Crystallogr. *66*, 213–221.

Albert, T.K., Hanzawa, H., Legtenberg, Y.I.A., de Ruwe, M.J., van den Heuvel, F.A.J., Collart, M.A., Boelens, R., and Timmers, H.T.M. (2002). Identification of a ubiquitin-protein ligase subunit within the CCR4-NOT transcription repressor complex. EMBO J. *21*, 355–364.

Bai, Y., Salvadore, C., Chiang, Y.C., Collart, M.A., Liu, H.Y., and Denis, C.L. (1999). The CCR4 and CAF1 proteins of the CCR4-NOT complex are physically and functionally separated from NOT2, NOT4, and NOT5. Mol. Cell. Biol. *19*, 6642–6651.

Basquin, J., Roudko, V.V., Rode, M., Basquin, C., Séraphin, B., and Conti, E. (2012). Architecture of the nuclease module of the yeast Ccr4-not complex: the Not1-Caf1-Ccr4 interaction. Mol. Cell *48*, 207–218.

Bawankar, P., Loh, B., Wohlbold, L., Schmidt, S., and Izaurralde, E. (2013). NOT10 and C2orf29/NOT11 form a conserved module of the CCR4-NOT complex that docks onto the NOT1 N-terminal domain. RNA Biol. *10*, 228–244.

Bhandari, D., Raisch, T., Weichenrieder, O., Jonas, S., and Izaurralde, E. (2014). Structural basis for the Nanos-mediated recruitment of the CCR4-NOT complex and translational repression. Genes Dev. *28*, 888–901.

Bhaskar, V., Roudko, V., Basquin, J., Sharma, K., Urlaub, H., Séraphin, B., and Conti, E. (2013). Structure and RNA-binding properties of the Not1-Not2-Not5 module of the yeast Ccr4-Not complex. Nat. Struct. Mol. Biol. *20*, 1281–1288.

Boland, A., Chen, Y., Raisch, T., Jonas, S., Kuzuoğlu-Öztürk, D., Wohlbold, L., Weichenrieder, O., and Izaurralde, E. (2013). Structure and assembly of the NOT module of the human CCR4-NOT complex. Nat. Struct. Mol. Biol. *20*, 1289–1297.

Braun, J.E., Huntzinger, E., Fauser, M., and Izaurralde, E. (2011). GW182 proteins directly recruit cytoplasmic deadenylase complexes to miRNA targets. Mol. Cell *44*, 120–133.

Chapat, C., and Corbo, L. (2014). Novel roles of the CCR4-NOT complex. Wiley Interdiscip. Rev. RNA *5*, 883–901.

Chekulaeva, M., Mathys, H., Zipprich, J.T., Attig, J., Colic, M., Parker, R., and Filipowicz, W. (2011). miRNA repression involves GW182-mediated recruitment of CCR4-NOT through conserved W-containing motifs. Nat. Struct. Mol. Biol. *18*, 1218–1226.

Chen, J., Rappsilber, J., Chiang, Y.C., Russell, P., Mann, M., and Denis, C.L. (2001). Purification and characterization of the 1.0 MDa CCR4-NOT complex identifies two novel components of the complex. J. Mol. Biol. *314*, 683–694.

Chen, Y., Boland, A., Kuzuoğlu-Öztürk, D., Bawankar, P., Loh, B., Chang, C.-T., Weichenrieder, O., and Izaurralde, E. (2014). A DDX6-CNOT1 complex and W-binding pockets in CNOT9 reveal direct links between miRNA target recognition and silencing. Mol. Cell *54*, 737–750.

Collart, M.A., and Struhl, K. (1994). NOT1(CDC39), NOT2(CDC36), NOT3, and NOT4 encode a global-negative regulator of transcription that differentially affects TATA-element utilization. Genes Dev. *8*, 525–537.

Cook, W.J., Jeffrey, L.C., Xu, Y., and Chau, V. (1993). Tertiary structures of class I ubiquitin-conjugating enzymes are highly conserved: crystal structure of yeast Ubc4. Biochemistry *32*, 13809–13817.

Cooper, K.F., Scarnati, M.S., Krasley, E., Mallory, M.J., Jin, C., Law, M.J., and Strich, R. (2012). Oxidative-stress-induced nuclear to cytoplasmic relocalization is required for Not4-dependent cyclin C destruction. J. Cell Sci. *125*, 1015–1026.

Cowtan, K. (2006). The Buccaneer software for automated model building. 1. Tracing protein chains. Acta Crystallogr. D Biol. Crystallogr. *62*, 1002–1011.

Daugeron, M.C., Mauxion, F., and Séraphin, B. (2001). The yeast POP2 gene encodes a nuclease involved in mRNA deadenylation. Nucleic Acids Res. *29*, 2448–2455.

Dimitrova, L.N., Kuroha, K., Tatematsu, T., and Inada, T. (2009). Nascent peptide-dependent translation arrest leads to Not4p-mediated protein degradation by the proteasome. J. Biol. Chem. *284*, 10343–10352.

Dominguez, C., Bonvin, A.M.J.J., Winkler, G.S., van Schaik, F.M.A., Timmers, H.T.M., and Boelens, R. (2004). Structural model of the UbcH5B/CNOT4 complex revealed by combining NMR, mutagenesis, and docking approaches. Structure *12*, 633–644.

Draper, M.P., Liu, H.Y., Nelsbach, A.H., Mosley, S.P., and Denis, C.L. (1994). Ccr4 is a glucose-regulated transcription factor whose leucine-rich repeat binds several proteins important for placing Ccr4 in its proper promoter context. Mol. Cell. Biol. *14*, 4522–4531.

Emsley, P., Lohkamp, B., Scott, W.G., and Cowtan, K. (2010). Features and development of Coot. Acta Crystallogr. D Biol. Crystallogr. *66*, 486–501.

Erben, E., Chakraborty, C., and Clayton, C. (2014). The CAF1-NOT complex of trypanosomes. Front. Genet. *4*, 299.

Evans, P.R., and Murshudov, G.N. (2013). How good are my data and what is the resolution? Acta Crystallogr. D Biol. Crystallogr. *69*, 1204–1214.

Fabian, M.R., Cieplak, M.K., Frank, F., Morita, M., Green, J., Srikumar, T., Nagar, B., Yamamoto, T., Raught, B., Duchaine, T.F., et al. (2011). miRNA-mediated deadenylation is orchestrated by GW182 through two conserved motifs that interact with CCR4-NOT. Nat. Struct. Mol. Biol. *18*, 1211–1217.

Fabian, M.R., Frank, F., Rouya, C., Siddiqui, N., Lai, W.S., Karetnikov, A., Blackshear, P.J., Nagar, B., and Sonenberg, N. (2013). Structural basis for the recruitment of the human CCR4-NOT deadenylase complex by tristetraprolin. Nat. Struct. Mol. Biol. *20*, 735–739.

Gulshan, K., Thommandru, B., and Moye-Rowley, W.S. (2012). Proteolytic degradation of the Yap1 transcription factor is regulated by subcellular localization and the E3 ubiquitin ligase Not4. J. Biol. Chem. *287*, 26796–26805.

Hanzawa, H., de Ruwe, M.J., Albert, T.K., van Der Vliet, P.C., Timmers, H.T., and Boelens, R. (2001). The structure of the C4C4 ring finger of human NOT4 reveals features distinct from those of C3HC4 RING fingers. J. Biol. Chem. *276*, 10185–10190.

Hodson, C., Purkiss, A., Miles, J.A., and Walden, H. (2014). Structure of the human FANCL RING-Ube2T complex reveals determinants of cognate E3-E2 selection. Structure *22*, 337–344.

Kabsch, W. (2010). XDS. Acta Crystallogr. D Biol. Crystallogr. *66*, 125–132.

Krissinel, E., and Henrick, K. (2007). Inference of macromolecular assemblies from crystalline state. J. Mol. Biol. *372*, 774–797.

Laribee, R.N., Shibata, Y., Mersman, D.P., Collins, S.R., Kemmeren, P., Roguev, A., Weissman, J.S., Briggs, S.D., Krogan, N.J., and Strahl, B.D. (2007). CCR4/NOT complex associates with the proteasome and regulates histone methylation. Proc. Natl. Acad. Sci. USA *104*, 5836–5841.

Lau, N.-C., Kolkman, A., van Schaik, F.M.A., Mulder, K.W., Pijnappel, W.W.M.P., Heck, A.J.R., and Timmers, H.T.M. (2009). Human Ccr4-not complexes contain variable deadenylase subunits. Biochem. J. *422*, 443–453.

Maillet, L., and Collart, M.A. (2002). Interaction between Not1p, a component of the Ccr4-not complex, a global regulator of transcription, and Dhh1p, a putative RNA helicase. J. Biol. Chem. *277*, 2835–2842.

Mathys, H., Basquin, J., Ozgur, S., Czarnocki-Cieciura, M., Bonneau, F., Aartse, A., Dziembowski, A., Nowotny, M., Conti, E., and Filipowicz, W. (2014). Structural and biochemical insights to the role of the CCR4-NOT complex and DDX6 ATPase in microRNA repression. Mol. Cell *54*, 751–765.

Matsuda, R., Ikeuchi, K., Nomura, S., and Inada, T. (2014). Protein quality control systems associated with no-go and nonstop mRNA surveillance in yeast. Genes Cells *19*, 1–12.

Mauxion, F., Prève, B., and Séraphin, B. (2013). C2ORF29/CNOT11 and CNOT10 form a new module of the CCR4-NOT complex. RNA Biol. *10*, 267–276.

McCoy, A.J., Grosse-Kunstleve, R.W., Adams, P.D., Winn, M.D., Storoni, L.C., and Read, R.J. (2007). Phaser crystallographic software. J. Appl. Crystallogr. *40*, 658–674.

Mersman, D.P., Du, H.-N., Fingerman, I.M., South, P.F., and Briggs, S.D. (2009). Polyubiquitination of the demethylase Jhd2 controls histone methylation and gene expression. Genes Dev. *23*, 951–962.

Mulder, K.W., Inagaki, A., Cameroni, E., Mousson, F., Winkler, G.S., De Virgilio, C., Collart, M.A., and Timmers, H.T.M. (2007a). Modulation of Ubc4p/Ubc5p-mediated stress responses by the RING-finger-dependent ubiquitin-protein ligase Not4p in *Saccharomyces cerevisiae*. Genetics *176*, 181–192.

Mulder, K.W., Brenkman, A.B., Inagaki, A., van den Broek, N.J.F., and Timmers, H.T.M. (2007b). Regulation of histone H3K4 tri-methylation and PAF complex recruitment by the Ccr4-Not complex. Nucleic Acids Res. *35*, 2428–2439.

Panasenko, O.O. (2014). The role of the E3 ligase Not4 in cotranslational quality control. Front. Genet. *5*, 141.

Panasenko, O.O., and Collart, M.A. (2011). Not4 E3 ligase contributes to proteasome assembly and functional integrity in part through Ecm29. Mol. Cell. Biol. *31*, 1610–1623.

Panasenko, O.O., and Collart, M.A. (2012). Presence of Not5 and ubiquitinated Rps7A in polysome fractions depends upon the Not4 E3 ligase. Mol. Microbiol. *83*, 640–653.

Panasenko, O., Landrieux, E., Feuermann, M., Finka, A., Paquet, N., and Collart, M.A. (2006). The yeast Ccr4-Not complex controls ubiquitination of the nascent-associated polypeptide (NAC-EGD) complex. J. Biol. Chem. *281*, 31389–31398.

Petit, A.P., Wohlbold, L., Bawankar, P., Huntzinger, E., Schmidt, S., Izaurralde, E., and Weichenrieder, O. (2012). The structural basis for the interaction between the CAF1 nuclease and the NOT1 scaffold of the human CCR4-NOT deadenylase complex. Nucleic Acids Res. *40*, 11058–11072.

Sandler, H., Kreth, J., Timmers, H.T.M., and Stoecklin, G. (2011). Not1 mediates recruitment of the deadenylase Caf1 to mRNAs targeted for degradation by tristetraprolin. Nucleic Acids Res. *39*, 4373–4386.

Suzuki, A., Igarashi, K., Aisaki, K.-I., Kanno, J., and Saga, Y. (2010). NANOS2 interacts with the CCR4-NOT deadenylation complex and leads to suppression of specific RNAs. Proc. Natl. Acad. Sci. USA *107*, 3594–3599.

Temme, C., Zhang, L., Kremmer, E., Ihling, C., Chartier, A., Sinz, A., Simonelig, M., and Wahle, E. (2010). Subunits of the drosophila CCR4-NOT complex and their roles in mRNA deadenylation. RNA *16*, 1356–1370.

Tucker, M., Staples, R.R., Valencia-Sanchez, M.A., Muhlrad, D., and Parker, R. (2002). Ccr4p is the catalytic subunit of a Ccr4p/Pop2p/Notp mRNA deadenylase complex in *Saccharomyces cerevisiae*. EMBO J. *21*, 1427–1436.

Wahle, E., and Winkler, S. (2013). RNA decay machines: deadenylation by the Ccr4-Not and Pan2-Pan3 complexes. Biochim. Biophys. Acta *1829*, 561–570.

Structure, Volume *23*

Supplemental Information

Architecture of the Ubiquitylation Module of the Yeast Ccr4-Not Complex

Varun Bhaskar, Jérôme Basquin, and Elena Conti

SUPPLEMENTAL FIGURES AND LEGENDS

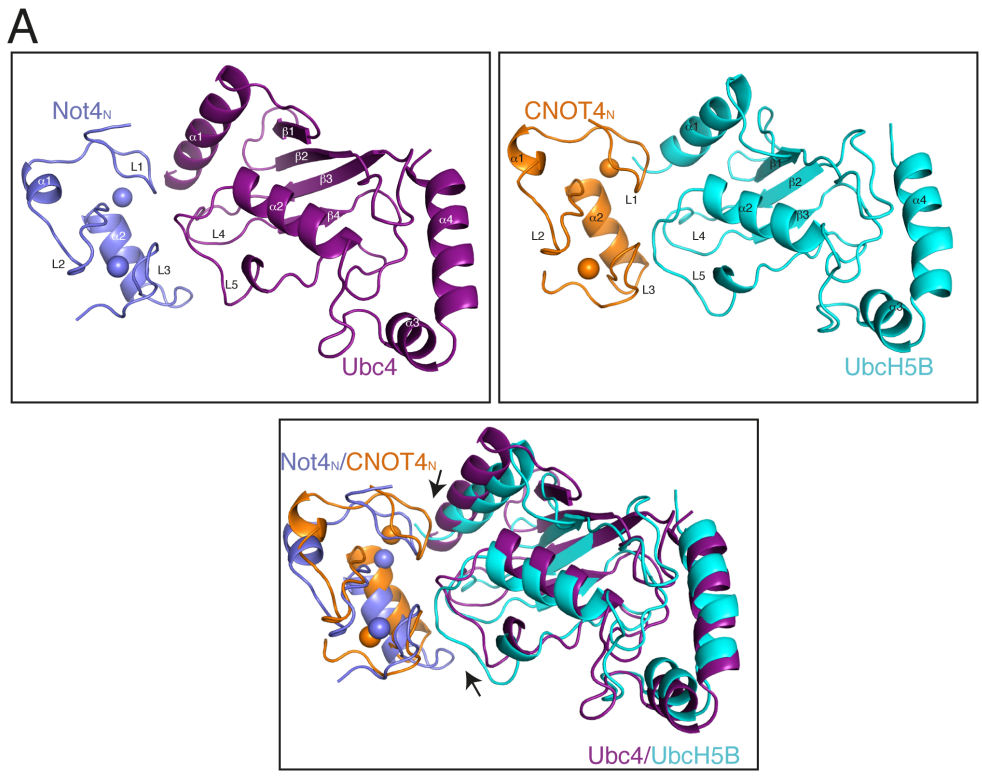

Figure S1

Detailed analysis of the Not4$_N$-Ubc4 crystal structure (Related to Figure 1)

(A) Not4$_N$-Ubc4 crystal structure and CNOT4-UbcH5B model are shown in similar orientation in the top panels. Superposition of the same is shown in the bottom panel. The difference in

the orientation of helix α1 of E2 and the loop regions of E3 at the interface are highlighted by arrows.

(B) Structure-based sequence alignment of all the E2 enzymes in *S. cerevisiae*. Not4 interacting residues of Ubc4 are indicated with blue dots. Residues providing specificity for this E2-E3 interaction are highlighted. The secondary structure elements are shown above the sequence.

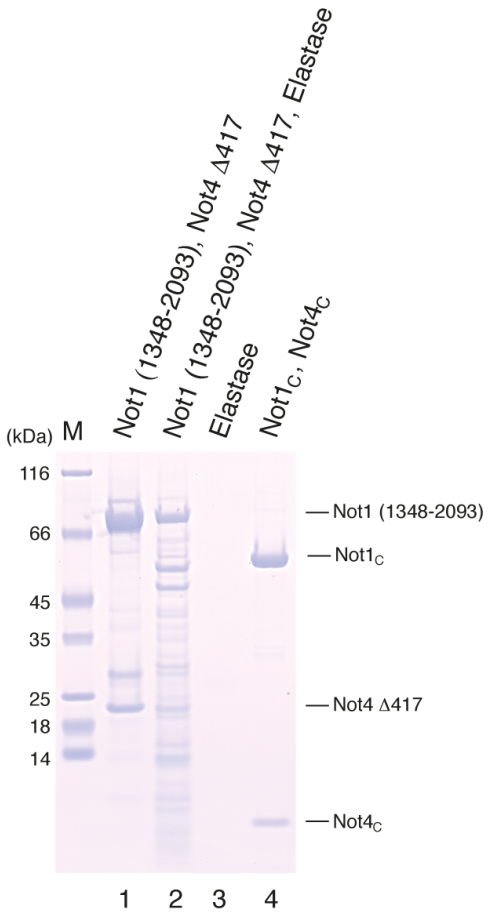

Figure S2

Identification of the $Not1_C$-$Not4_C$ minimal complex (Related to Figure 2)

Not1 (1348-2093)-Not4 Δ417 complex is shown in lane1. Limited proteolysis of Not1 (1348-2093)-Not4 Δ417 was carried out by incubating the complex at 0.6 mg ml^{-1} with elastase (Roche) for 60 minutes on ice at an enzyme to protein ratio of 1:10 and is shown in lane2. The mixture was then subjected to size-exclusion chromatography in a buffer containing 20 mM Tris-Cl pH 7.5, 250 mM NaCl and 2 mM DTT. The peaks were analyzed on 4-12% Bis-Tris NuPage gel with MES-SDS as the running buffer. The interacting fragments were identified by N-terminal sequencing and Liquid chromatography-Mass spectrometry (LC-MS) analysis. $Not1_C$-$Not4_C$ complex that was used for structural studies is shown in lane4.

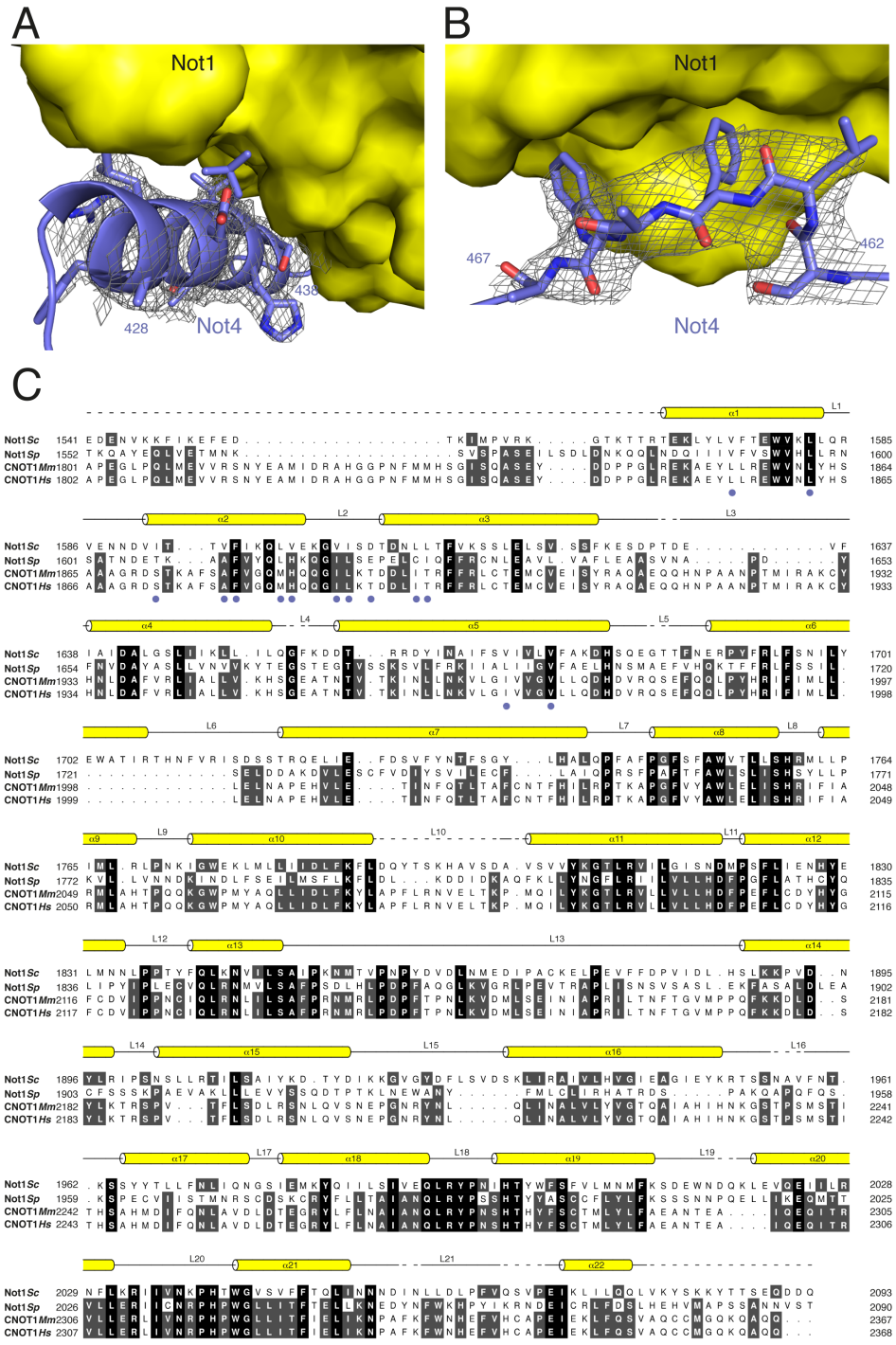

Figure S3

Detailed analysis of the Not1$_C$-Not4$_C$ crystal structure (Related to Figure 3)

(A-B) 2F_O-F_C electron density of Not4$_C$ at the hydrophobic interaction segments contoured at 0.9σ (corresponding to Figure 3A and 3C).

(C) Structure-based sequence alignment of Not1$_C$ from different species, including *S. cerevisiae* (*Sc*), *M. musculus* (*Mm*) and *H. sapiens* (*Hs*), highlighting the interacting residues with blue dots. The secondary structure elements are shown above the sequence.

SUPPLEMENTAL EXPERIMENTAL PROCEDURE

Protein purification

All proteins were cloned and expressed in *E. coli* BL21 pLysS cells (Stratagene) in TB medium with 0.5 mM IPTG induction overnight at 18 ˚C. Not1 constructs were expressed as previously described in (Bhaskar et al., 2013). $Not4_N$ and full-length Ubc4 were expressed as a fusion protein (connected by the linker TGSTGSTETG) with a N-terminal His-SUMO tag cleavable by Senp2 protease. The $Not4_C$, $Not4_C$–ΔN and $Not4_C$–ΔC (Not4 residues 418-477, 442-477 and 418-462, respectively) constructs were expressed as N-terminal His-GST fusion proteins followed by a 3C cleavage site. The proteins were purified using similar protocols as previously described (Bhaskar et al., 2013). Briefly, a first step of Nickel-based affinity chromatography was followed by tag cleavage and size-exclusion chromatography. For pull-down experiments, the GST-tagged proteins were purified with the same protocol but omitting the tag cleavage step.

Crystallization

The $Not4_N$-Ubc4 complex was crystallized at 48 mg ml^{-1} by vapour diffusion using 10% (w/v) PEG 8000, 0.02 M L-Na-Glutamate, 0.02 M Alanine (racemic), 0.02 M Glycine, 0.02 M Lysine HCl (racemic), 0.02 M Serine (racemic), 0.1 M Bicine/Tris-Cl pH 8.5 and 20% (w/v) ethylene glycol as crystallization buffer at room temperature.

$Not1_C$-$Not4_C$ complex was crystallized at 12 mg ml^{-1} by vapour diffusion using 10% (w/v) PEG 4000, 0.02 M 1,6-Hexanediol, 0.02 M 1-Butanol, 0.02 M 1,2-Propanediol (racemic), 0.02 M 2-Propanol, 0.02 M 1,4-Butanediol, 0.02 M 1,3-Propanediol, 0.1 M MOPS/Hepes-Na 7.5 and 20% Glycerol as crystallization buffer at room temperature.

Pull-down assays

100 pmol of GST-tagged protein was incubated with 200 pmol of the untagged prey protein for 1hr at 4 ˚C in the binding buffer (BB150 – 20 mM Tris-Cl pH 7.5, 150 mM NaCl, 2 mM DTT, 12.5% (v/v) glycerol and 0.1% (w/v) NP40). 400 µL of BB150 buffer and 20 µL of 50% GSH-Sepharose resin were added to the protein mix and incubated for 1 hr with gentle rocking at 4 ˚C. The resin was washed 3 times with BB150 and the proteins were eluted with 15 µL of BB150 containing 20 mM Glutathione. Input and precipitate were mixed with 3X SDS loading dye and resolved on 4-12% Bis-Tris NuPage gel (Invitrogen) using MES-SDS as running buffer, and visualized by Coomassie blue staining.